An Infrared Thermography Based Quantification Method of Two-Phase Refrigerant Distribution in Brazed Plate Heat Exchangers

Wenzhe Li
University of Illinois at Urbana and Champaign, liwz310@illinois.edu

Pega Hrnjak
University of Illinois at Urbana and Champaign

An infrared thermography based quantification method of two-phase refrigerant distribution in brazed plate heat exchangers

Wenzhe LI[1], Pega HRNJAK[1,2]*

[1]ACRC, the University of Illinois,
Urbana, Illinois, USA
liwz310@illinois.edu, pega@illinois.edu

[2]Creative Thermal Solutions In. (CTS),
Urbana, Illinois, USA

* Corresponding Author

ABSTRACT

When used as direct expansion (DX) evaporators, brazed plate heat exchangers (BPHEs) suffer from the maldistribution of the two-phase refrigerant among parallel plate channels. It is essential to accurately quantify the two-phase refrigerant distribution in BPHEs to evaluate the effect of the maldistribution on the heat exchangers and system performance. Considering the complex internal geometry of BPHEs and the potential influence of experimental measurements on the original flow field, the non-intrusive quantification of the two-phase flow distribution in BPHEs is preferred.

This paper presents a method to quantify the two-phase refrigerant distribution in BPHEs from infrared images. Quantification is achieved by identifying the boundary between the two-phase and superheated region on the sidewall of BPHEs based on the infrared images and matching the identified boundary in a BPHE evaporator model to estimate the two-phase distribution.

The proposed quantification method is validated by the experimental data. The results show that this non-intrusive method can effectively quantify the two-phase refrigerant distribution in the BPHE.

1. INTRODUCTION

When used as direct expansion (DX) evaporators, brazed plate heat exchangers (BPHEs) suffer from the maldistribution of the two-phase refrigerant among parallel plate channels. It is essential to accurately quantify the two-phase refrigerant distribution in BPHEs to evaluate the effect of the maldistribution on the heat exchanger and system performance.

In the past two decades, many experimental approaches have been developed in the literature to quantify the two-phase flow distribution in the heat exchangers with the “headers and multi-parallel channels” structure, like microchannel heat exchangers (MCHXs) and plate heat exchangers (PHEs) with different types: frame-type, brazed-type, and shell-type. Generally, quantification methods can be divided into two categories: direct measurement and indirect quantification. Many researchers made the effort to directly measure the two-phase flow distribution. Osakabe et al. (1999) studied the distribution of air and water flow in a horizontal manifold with upward flow tubes. The water flow distribution was measured by separating the two phases at downstream of each branch. Fei and Hrnjak (2002) experimentally quantified the two-phase flow of R134a in the inlet header of an automotive PHE with downward flow channels. In their study, the flow rate distribution of vapor and liquid refrigerant was measured after the two phases were separated for each channel. Two years later, Vist and Peterson (2004) proposed an experimental method to measure the two-phase R134a distribution in a PHE inlet header with the diabatic conditions for the tubes. In the tests, the authors isolated the two-phase flow of one tube at a time and condensed the refrigerant into a subcooling state to measure the flow rate. The vapor quality at the inlet of each tube was then estimated by the energy balance. The two-phase flow distributions of 5 different refrigerants (R245fa, R134a, R410A, and R32) in a vertical header of MCHXs were investigated by Zou and Hrnjak (2014). In their experiments, the two-phase refrigerant was heated to be superheated in each microchannel to measure the flow rate and the inlet vapor quality was obtained by the energy balance of each microchannel. More recently, Mahvi and Garimilla (2019) developed an in-channel thermal flow meter to explore the two-phase R134a flow distribution in a rectangular header with downward flow tubes. The developed thermal flow meter measured the flow rate of the subcooled refrigerant based on the difference in the propagating time of the upstream generated pulse thermal signal to the two thermocouples at downstream. As for the indirect quantification, Li and Hrnjak (2015) developed a method to quantify the distribution of liquid refrigerant in a real MCHX from infrared images. Quantification was achieved by building the relationship between the liquid mass flow rate through each microchannel tube and the air-side capacity calculated from the infrared measurement of the wall temperature. The vapor refrigerant distribution was then estimated by implementing the liquid refrigerant distribution into a heat exchanger model.

Considering the complex internal geometry of BPHEs, it is difficult to directly measure the two-phase flow rate in the plate channels. Moreover, indirect quantification has the advantage of non-intrusive, which is preferred for BPHEs.

This paper presents a method to quantify the two-phase refrigerant distribution in BPHEs from infrared images. Quantification is achieved by identifying the boundary between the two-phase and superheated region on the sidewall of BPHEs based on the infrared images and matching the identified boundary in a BPHE evaporator model to estimate the two-phase distribution. The proposed quantification method is validated by the experimental results.

2. EXPERIMENTAL FACILITY

The experimental facility is shown in Fig. 1. In the tests, distilled water, heated by two immersion electrical heaters in the tank, is circulating through one side of the tested BPHE to provide heat to the refrigerant. The subcooled refrigerant, R134a, is driven by a gear pump and the flow rate is measured by a Coriolis type mass flow meter. The refrigerant is then heated into a desirable vapor quality and becomes fully developed in a transparent developing tube before the tested BPHE. The two-phase refrigerant enters the BPHE through the inlet header at the bottom and then is distributed into different plate channels. The refrigerant absorbs heat from the water and evaporates in the plate channels. An infrared camera is used to capture the temperature profile on the sidewalls of the BPHE. After evaporation, the refrigerant leaves the BPHE through the outlet header at the top and flows through the condenser and subcooler to ensure a subcooled state before the pump. The pressure transducers and type T (copper-constantan) thermocouples are installed at the locations indicated in Fig 1. Four probes are inserted into the headers of the tested BPHE to measure the pressure profile in the headers and the temperature change across the plate channels. Details of the probe design can be found in Li and Hrnjak (2021a). In this study, a BPHE with 50 plates is used, of which the geometric parameters are listed in Table 1.

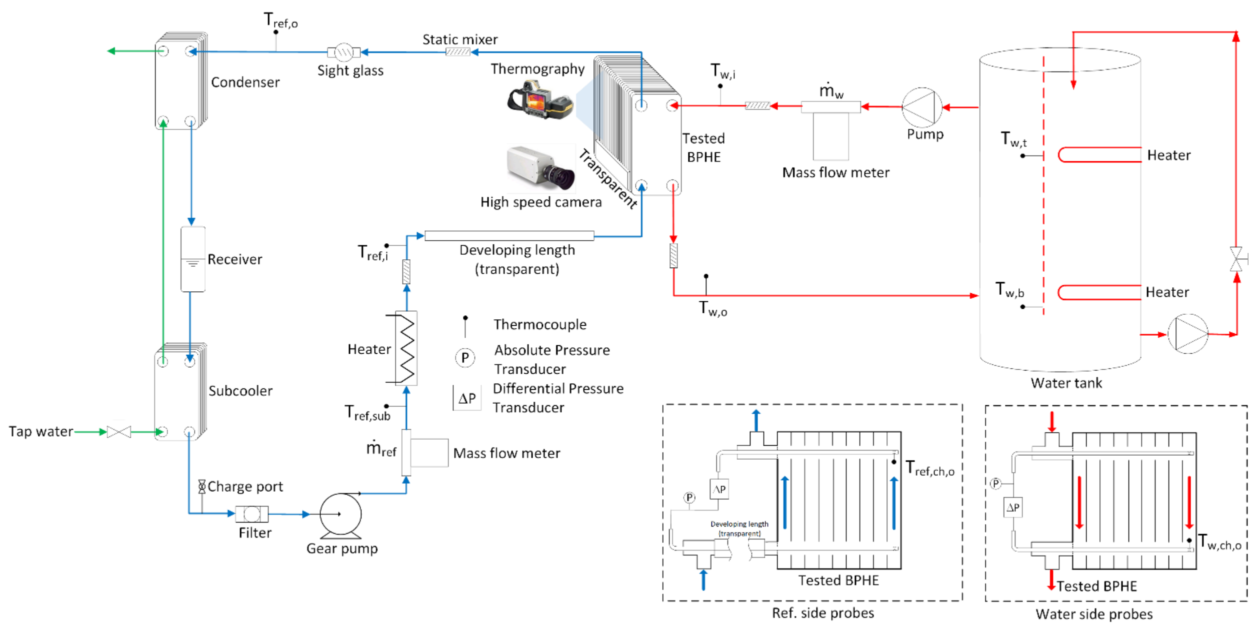

Figure 1: Experimental facility

The calibration tests have been performed to correct the temperature measurements of the infrared camera. Before the calibration, a thin layer of flat black paint was sprayed on the sidewall to increase the emissivity of the surface ($\varepsilon \approx 0.94$). In the calibration, the refrigerant side was evacuated and the high mass flow rate of water at a certain temperature was supplied to the water side. Such an arrangement guaranteed a uniform temperature profile on the sidewall. A calibrated thermocouple was attached to the sidewall of the BPHE by the aluminum tape and the thermal paste was applied to fill the gap between the wall and the thermocouple. At different water temperatures, the temperature of the sidewall measured by the infrared camera, and that by the thermocouple, was compared and a calibration equation was obtained by the linear fitting to correct the readings of the infrared camera. The same procedure was applied to the sidewall near the refrigerant ports and the water ports.

Table 1: Geometric parameters of the BPHE

Parameter	Value
Chevron angle, φ, ^{o}	60
Corrugation depth, b, mm	2.0
Corrugation pitch, P_c, mm	7.0
Plate thickness, t, mm	0.30
Port length, L_p, mm	172
Total length, L_v, mm	206
Port width, L_h, mm	42
Total width, L_w, mm	76
Heat transfer area per plate, A_p, m^2	0.014
Port diameter, D_p, mm	20.0

3. QUANTIFICATION METHOD

3.1 Identification of the boundary between the two-phase and superheated region from the IR images

As mentioned above, the quantification requires the identification of the boundary between the two-phase and superheated region on the sidewall from the IR images. Fig. 2 gives the IR image of the sidewall near the water ports at a certain experimental condition ($G_{r,i}$ = 76.8 kg/m^{2}s, $x_{r,i}$ = 0.1, $T_{r,sat}$ = 15.3 ^{o}C, $T_{w,i}$ = 30.0 ^{o}C, $G_{w,i}$ = 400.6 kg/m^{2}s). The two-phase and superheated regions can be identified from this IR image: the two-phase region is at the bottom with a lower wall temperature and the superheated region is at the top with a higher wall temperature. The length of the two-phase and superheated region in the plate length direction is different along the heat exchanger depth, which indicates the two-phase maldistribution in the BPHE. Moreover, the water channel and refrigerant channel are not distinguishable in the IR image. This is due to the complex channel geometry and the heat conduction of the sidewall.

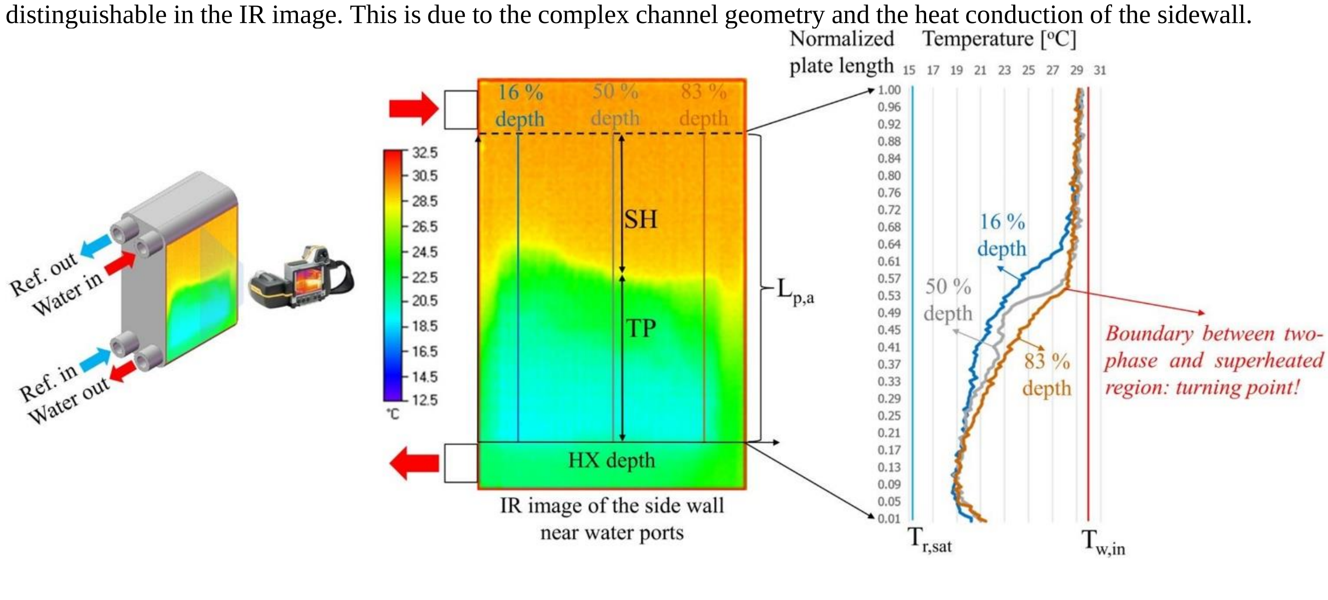

Figure 2: IR image of the sidewall near the water ports

The temperature profiles along the plate length direction (vertical) at three different locations in the heat exchanger depth are also plotted in Fig. 2. The temperature profiles show that, in the superheated region, the surface temperature of the sidewall is almost constant and quite close to the water inlet temperature ($T_{w,i}$). This is because, on one hand, water has a relatively large specific heat, so the temperature change of the water in the superheated region is quite small; on the other hand, the heat transfer coefficient of water (~2000 W/m^{2}K) is much larger than that of the superheated refrigerant (~300 W/m^{2}K), so the sidewall temperature is very close to the water temperature. In the two-phase region at the bottom, the temperature profiles show an increasing trend along the plate length, and the lowest temperature is higher than the saturation temperature of refrigerant ($T_{r,sat}$). This is because, in the two-phase region, the heat transfer coefficient of water and the refrigerant is comparable thus the sidewall temperature is equivalently determined by both the water side and refrigerant side temperature profile. It can be inferred from the analysis and the boundary between the two-phase and superheated region is the turning point of the temperature profile.

To locate the turning point, the temperature profile is first smoothed and the triangle thresholding method is used. In this method, a straight line is connected to the highest and lowest temperature point in the profile and the turning point is where the perpendicular distance between the straight line and the temperature curve reaches its maximum, as demonstrated in Fig. 3. Identifying the turning point for all columns in the IR image, the boundary between the two-phase and superheated region is thereby obtained.

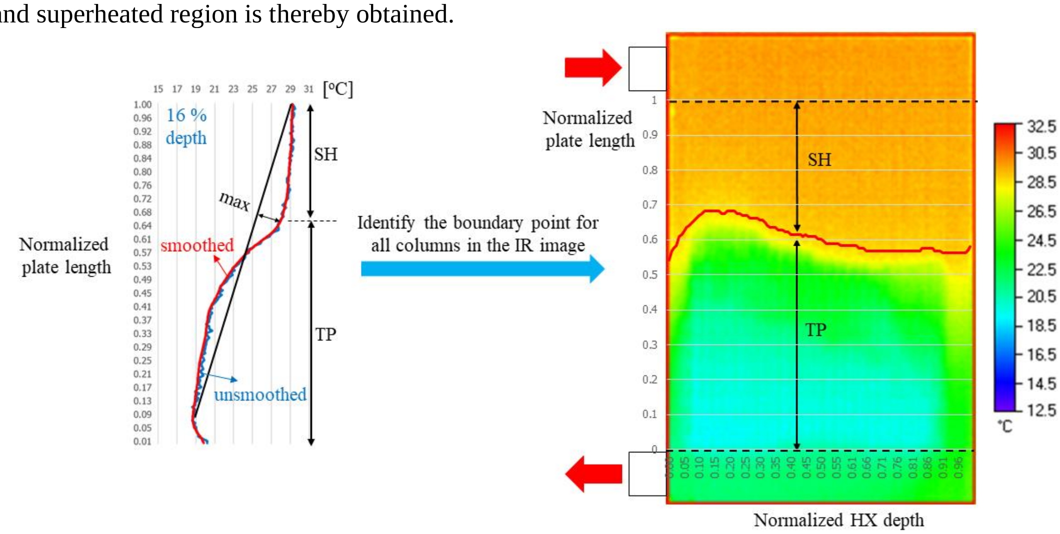

Figure 3: Identification of the boundary between the two-phase and superheated region

The same procedure is applied to the IR image of the sidewall near the refrigerant ports and the identified boundaries from the two sidewalls are compared in Fig. 4. The two boundaries are similar but not identical. The difference between the two boundaries is the result of the two-phase maldistribution within the plate channel. An averaged boundary is then obtained as a 1-D approximation.

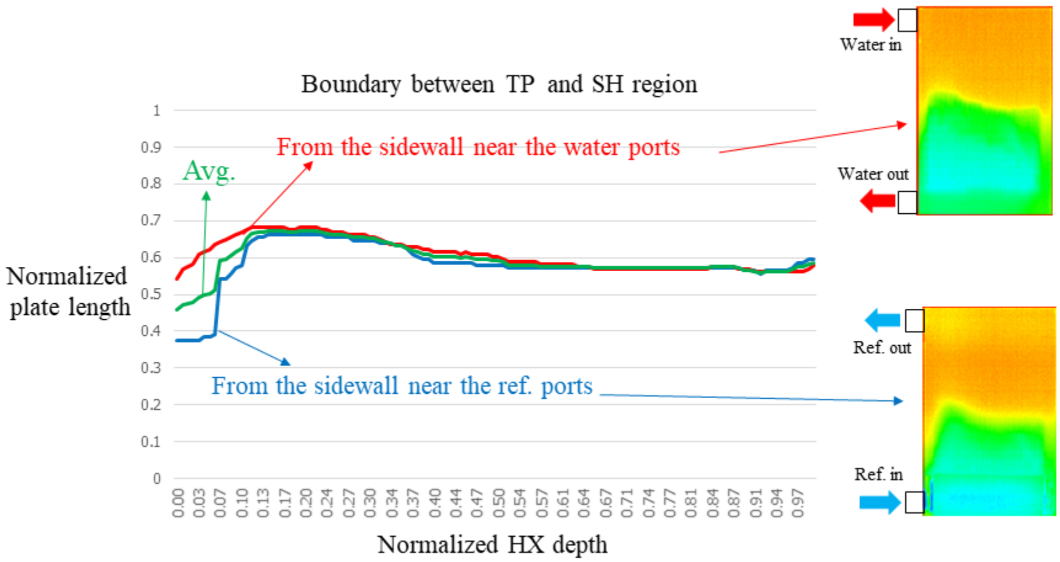

Figure 4: Comparison of the boundary between the two-phase and superheated region, obtained from two sidewalls

3.2 BPHE Evaporator Model

This quantification approach estimates the two-phase refrigerant distribution with the corporation of a BPEH evaporator exchanger model. Several assumptions are made in the development of this BPHE evaporator model: (1) fluids are 1-D flow along the plate length direction; (2) heat transfer along the fluids flowing direction is neglected; (3) the thermal resistance of the metal plates is neglected; (4) the end-plate effect is neglected; (5) flows in the inlet/outlet headers are adiabatic; (6) refrigerant flow in the outlet header is homogenous.

3.2.1 Principle of equal total pressure drop

This BPHE evaporator model takes the liquid refrigerant distribution, which is estimated based on IR images of the sidewalls, as the input to calculate the vapor refrigerant distribution and predict the overall performance of the heat exchanger. The basic principle is to adjust the vapor refrigerant distribution to achieve an equal total pressure drop for all flow paths starting at the entrance and ending at the exit of the heat exchanger, as shown in Fig. 5. For each flow path, the total pressure drop is divided into three components: the pressure drop in the inlet/outlet header and that across the plate channel:

$$\Delta P_{path,i} = \sum_{1}^{i} \Delta P_{in-hd,i} + \Delta P_{ch,i} + \sum_{1}^{i} \Delta P_{out-hd,i} \tag{1}$$

Two components are accounted for the pressure drop in the inlet/outlet header: frictional and acceleration/deceleration pressure drop:

$$\Delta P_{in/out-hd,i} = \Delta P_{fri,hd} + \Delta P_{acc/decc,hd} \tag{2}$$

The pressure drop across the plate channel includes: local pressure drop of turning-in and turning-out, frictional, gravitational, and acceleration pressure drop:

$$\Delta P_{ch,i} = \Delta P_{turn-in,i} + \Delta P_{fri,i} + \Delta P_{gra,i} + \Delta P_{acc,i} + \Delta P_{turn-out,i} \tag{3}$$

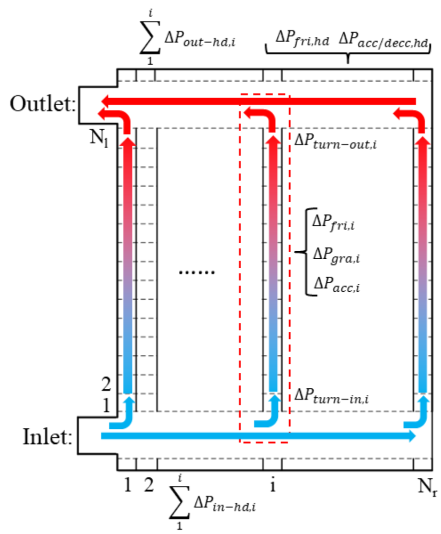

Figure 5: Flow paths and total pressure drop calculation in BPHEs

3.2.2 In-channel heat transfer calculation

In a BPHE, one interior channel is directly transferring heat with two adjacent channels in a counterflow arrangement. Therefore, the temperature profiles of the refrigerant side and water side are mutually dependent, and the iteration is needed for the calculation. In this model, the finite volume approach is used to calculate the in-channel heat transfer and pressure drop. Each channel is discretized into several layers or elements in the plate length direction. The in-channel heat transfer calculation algorithm is given in Fig. 6. The temperature profile of the water side is first initialized and fixed. The heat transfer and pressure drop of the refrigerant flow in each channel are calculated along the flowing direction (upward). The water side temperature profile is then updated based on the previously calculated heat transfer results and the update is along the water flowing direction (downward). Then, the next round of the refrigerant side calculation starts, and the iteration continues until the temperature profile of both sides stabilizes. Besides, the water flow in the other side of the BPHE is also maldistributed and such a maldistribution affects the refrigerant side distribution through heat transfer. To account for this effect, an experimentally validated model proposed in Li and Hrnjak (2021a) is used to predict the single-phase water flow distribution in the BPHE.

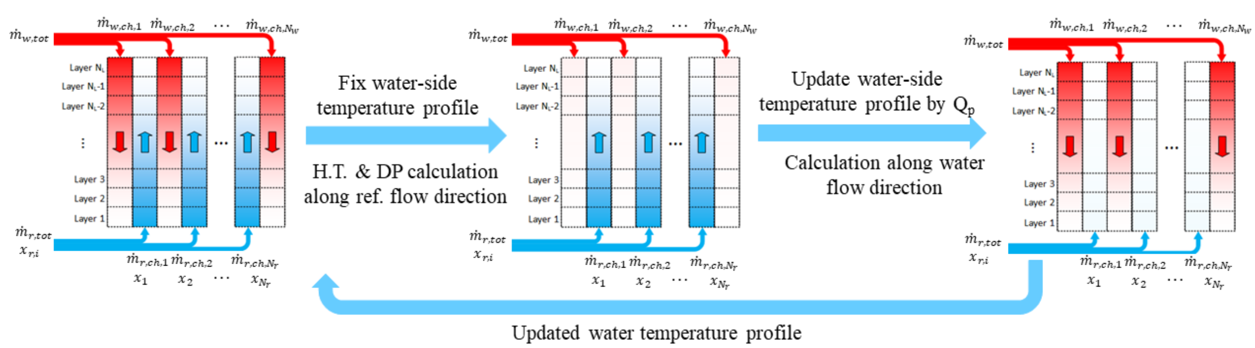

Figure 6: In-channel heat transfer calculation algorithm

For each element in the refrigerant side, the total heat transfer is the summation of the heat transfer from two adjacent plates, which is calculated by the UA-LMTD method separately:

$$\dot{m}_{r,ch,\,j} \cdot \Delta h_r(i,j) = U_{left} \cdot LMTD_{left} \cdot A_L + U_{right} \cdot LMTD_{right} \cdot A_L \tag{4}$$

For the heat transfer and pressure drop calculation, the correlations from the literature are applied, depending on the flow conditions. Table 2 summarizes the selected correlations.

Table 2: Summary of selected correlations

Items	**Correlations**
Water side (in-channel)	
Heat transfer coefficient	Li and Hrnjak (2021b)

Refrigerant side (in-channel)	
Single-phase heat transfer coefficient	Li and Hrnjak (2021b)
Single-phase frictional pressure drop	Li and Hrnjak (2021a)
Two-phase heat transfer coefficient Two-phase frictional pressure drop	Almalfi et al. (2016)
Void fraction	Rouhani and Axelson (1970)
Gravitational pressure drop	Homogeneous model
Acceleration pressure drop	Homogeneous model
Local turning-in pressure loss	Buell et al. (1994)
Local turning-out pressure loss	Collier and Thome (1994)
Refrigerant side (inlet header)	
Frictional pressure drop	Friedel (1970)
Deceleration pressure drop	Buell et al. (1994)
Refrigerant side (outlet header)	
Frictional pressure drop	Homogeneous model + Blasius correlation
Acceleration pressure drop	Homogeneous model

3.2.3 Iteration algorithm for the entire BPHE

The iteration algorithm for the entire BPHE is shown in Fig. 7. For a given inlet condition and a certain liquid refrigerant distribution obtained from the IR images, the iteration starts by initializing or guessing a vapor refrigerant distribution. Then, the in-channel heat transfer and pressure drop are calculated as described in 3.2.2. The total pressure drop of each flow path is next estimated based on the discussion in 3.2.1. If the total pressure drop of each flow path is not identical, then the vapor refrigerant distribution is adjusted based on the calculated total pressure drop to start a new iteration. The iteration continues until the total pressure drop for each flow path is equal. After the iteration, the vapor refrigerant distribution and the overall performance of the heat exchanger are thereby obtained.

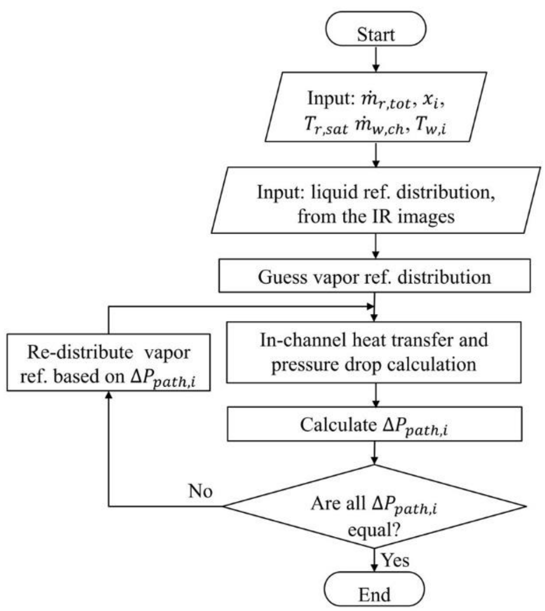

Figure 7: Iteration algorithm for the entire BPHE

3.3 Solving for the two-phase refrigerant distribution

An algorithm (shown in Fig. 8) is developed to solve for the two-phase refrigerant distribution in the BPHE based on the boundary obtained in 3.1, with the corporation of the BPHE evaporator model.

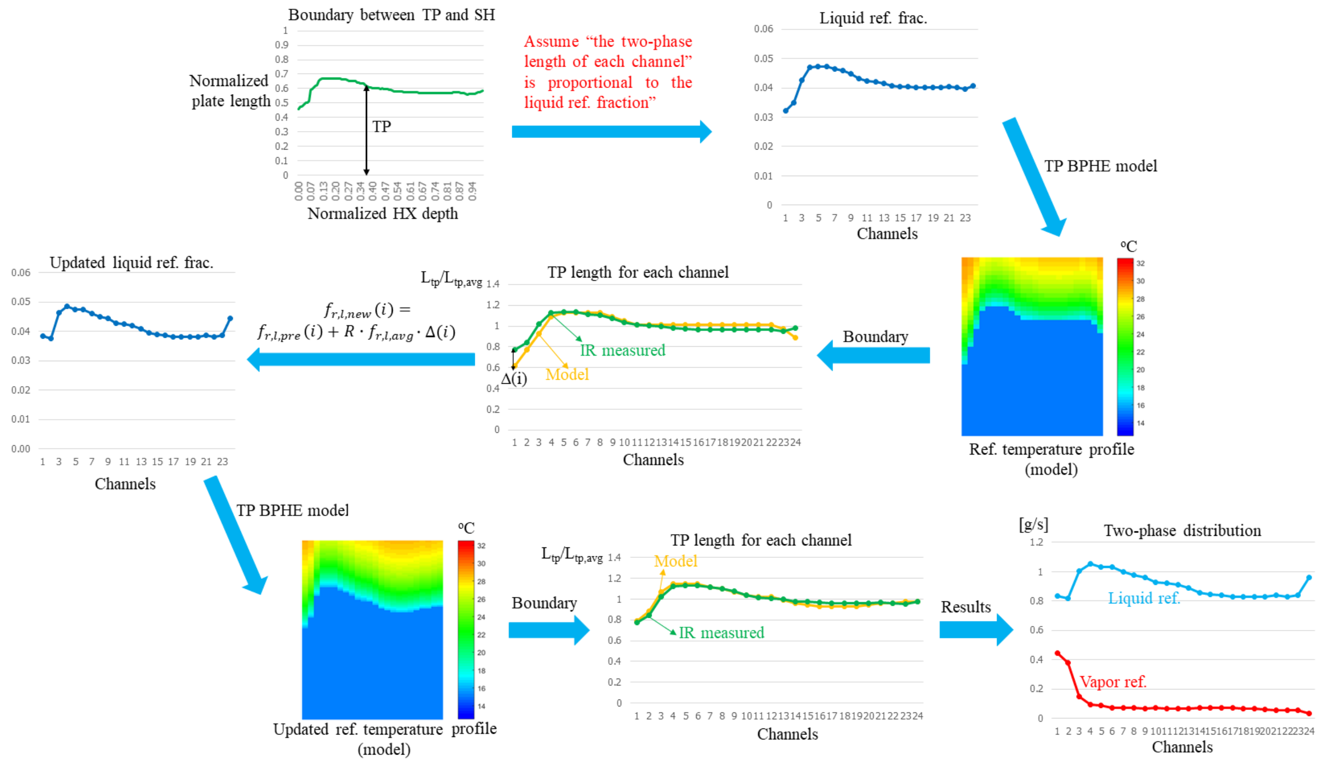

Figure 8: Algorithm of solving the two-phase refrigerant distribution in BPHEs

This algorithm starts by assuming "the two-phase length of each channel is proportional to the inlet liquid refrigerant fraction in each channel" and a liquid refrigerant distribution can be calculated from the boundary identified in 3.1. This calculated liquid refrigerant distribution is then inputted into the BPHE evaporator model described in 3.2, which outputs the vapor refrigerant distribution and the prediction of the overall performance of the heat exchanger. Then, the predicted two-phase length of each plate channel is compared with the IR measured value. The difference between the measured and predicted two-phase length is caused by the inaccurate liquid refrigerant distribution. The following equation is then used to correct the liquid refrigerant distribution:

$$f_{r,l,new}(i) = f_{r,l,pre}(i) + R \cdot f_{r,l,avg} \cdot \Delta(i) \tag{5}$$

In the above equation, $f_{r,l,pre}(i)$ and $f_{r,l,new}(i)$ is the previous and updated liquid refrigerant fraction, R is a relaxation factor, $f_{r,l,avg}$ is the averaged liquid refrigerant fraction and $\Delta(i)$ is the difference between the measured and calculated two-phase length in a non-dimensional form. With the updated liquid refrigerant distribution, the two-phase length of each channel is then updated by the BPHE evaporator model and compared with the IR measured value again. The iteration continues until the calculated two-phase length of each channel is the same as the measured. Finally, the two-phase refrigerant distribution, as well as the overall performance of the BPHE, is obtained.

4. METHOD VALIDATION

The experimental results are used to validate the newly proposed quantification method. The experiments covered three different refrigerant inlet vapor quality ($x_{r,i}$ ~ 0.1, 0.2, 0.3) and three different refrigerant mass flux at the BPHE inlet ($G_{r,i}$ ~ 77, 96.3, 115.5 kg/m^{2}s). In the tests, the saturation temperature of the refrigerant ($T_{r,sat}$) and the inlet temperature of the water ($T_{w,i}$) is maintained around 15 and 30 ^{o}C respectively. The water mass flux at the BPHE inlet is changing proportionally to the refrigerant mass flux. The resulting bulk exit superheat of refrigerant is ranging from 8 to 13 ^{o}C.

This quantification method estimates the two-phase refrigerant distribution and simultaneously predicts the overall performance of the BPHE. Fig. 9 shows the comparison of the measured and predicted heat exchanger capacity. It can be seen from Fig. 9, the experimental and modeling results agree well with each other.

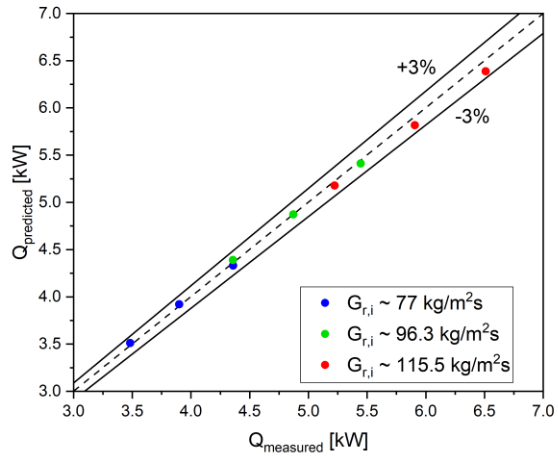

Figure 9: BPHE capacity validation

Another validation is the pressure profile in the inlet/outlet header of the BPHE. In the experiments, by moving the pressure probes, the pressure profile in the header is measured. In the proposed quantification method, the accurate prediction of the pressure profile in the headers is crucial for the determination of the vapor refrigerant distribution. Good agreements between the measured and predicted results at different test conditions are achieved as shown in Fig. 10.

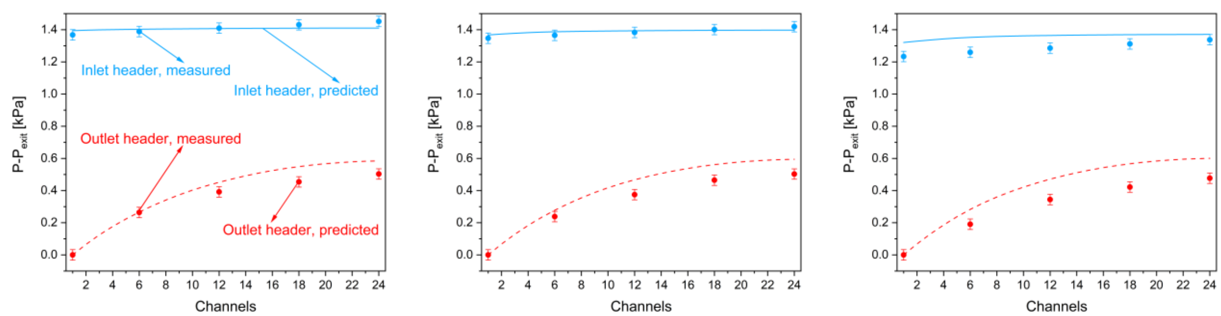

$G_{r,i}$ ~ 115.5 kg/m^{2}s, $x_{r,i}$ ~ 0.1 $G_{r,i}$ ~ 115.5 kg/m^{2}s, $x_{r,i}$ ~ 0.2 $G_{r,i}$ ~ 115.5 kg/m^{2}s, $x_{r,i}$ ~ 0.3

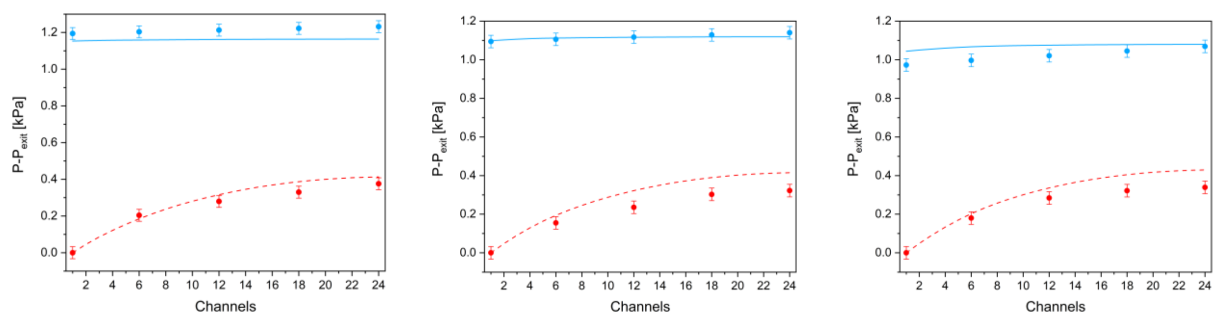

$G_{r,i}$ ~ 96.3 kg/m^{2}s, $x_{r,i}$ ~ 0.1 $G_{r,i}$ ~ 96.3 kg/m^{2}s, $x_{r,i}$ ~ 0.2 $G_{r,i}$ ~ 96.3 kg/m^{2}s, $x_{r,i}$ ~ 0.3

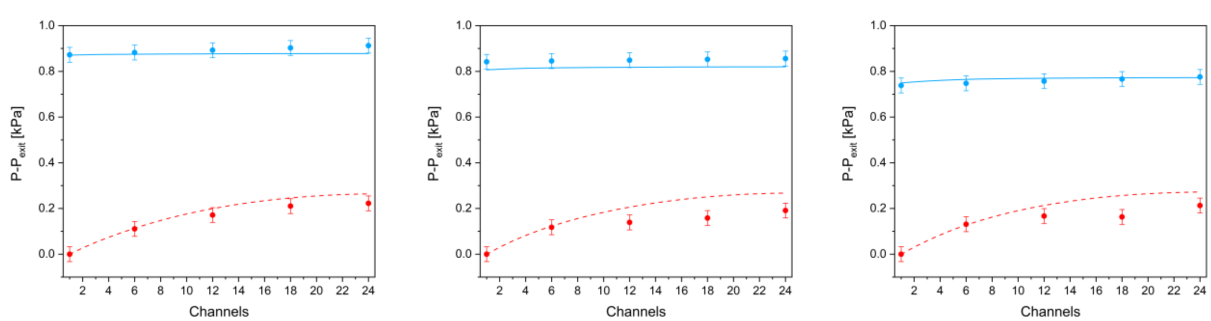

$G_{r,i}$ ~ 77 kg/m^{2}s, $x_{r,i}$ ~ 0.1 $G_{r,i}$ ~ 77 kg/m^{2}s, $x_{r,i}$ ~ 0.2 $G_{r,i}$ ~ 77 kg/m^{2}s, $x_{r,i}$ ~ 0.3

Figure 10: pressure profile validation

5. CONCLUSION

In this study, an IR thermography-based method is proposed to quantify the two-phase refrigerant distribution in BPHEs. In this method, the boundary between the two-phase and superheated region on the sidewall of the BPHE is first identified from the IR image. The identified boundary is then matched in a BPHE evaporator model by adjusting the two-phase distribution. The quantification of the two-phase distribution is thereby achieved. The overall performance of the BPHE is simultaneously predicted in the quantification. The proposed quantification method is validated by the measured BPHE capacities and the pressure profiles in the headers of the BPHE.

NOMENCLATURE

A_L	layer heat transfer area	kg m^{-2} s
f	liquid fraction	-
G	mass flux	kg m^{-2} s
h	enthalpy	J kg^{-1} K^{-1}
L	length	m
LMTD	log-mean temperature difference	ºC
$\dot{m}$	mass flow rate	kg s^{-1}
P	pressure	kPa
Q	Heat exchanger capacity	kW
R	relaxation factor	-
SH	superheat	-
T	temperature	ºC
TP	two-phase	-
U	overall heat transfer coefficient	W m^{-2} K^{-1}
x	vapor quality	-

Subscript

avg	average
ch	channel
hd	header
l	liquid
o	outlet
i/in	inlet
r	refrigerant
sat	saturation
tot	total
tp	two-phase
w	water

REFERENCES

Amalfi, R. L., Vakili-Farahani, F. & Thome, J. R. (2016). Flow boiling and frictional pressure gradients in plate heat exchangers. Part 2: Comparison of literature methods to database and new prediction methods. *International Journal of Refrigeration*, 61, 185–203.
Buell, J. R., Soliman, H. M. & Sims, G. E. (1994). Two-phase pressure drop and phase distribution at a horizontal tee junction. *International Journal of Multiphase Flow*, 20(5), 819-836.
Collier, J.G., Thome, J.R. (1994). *Convective Boiling and Condensation (3rd Eds)*. Oxford University Press, Oxford, U.K.
Fei, P., Cantrak, D., & Hrnjak, P. (2002). Refrigerant distribution in the inlet header of plate evaporators. *Proceedings of the SAE World Congress*, Detroit, MI, Paper 2002-01-0948.
Friedel, L. (1979). Improved friction pressure drop correlations for horizontal and vertical two-phase pipe flow. *Proceedings of the European Two Phase Flow Group Meeting, Ispra, Italy*, paper E2.

Li, H., Hrnjak, P. (2015). Quantification of liquid refrigerant distribution in parallel flow microchannel heat exchanger using infrared thermography. *Applied Thermal Engineering*, 78, 410-418.

Mahvi, A. J., Garimella, S. (2019). Two-phase flow distribution of saturated refrigerants in microchannel heat exchanger headers. *International Journal of Refrigeration*, 104, 84–94.

Li, W., Hrnjak, P. (2021a). Single-phase flow distribution in plate heat exchangers: experiments and models. *International Journal of Refrigeration*, In Press.

Li, W., Hrnjak, P. (2021b). Compensating for the end-plate effect on heat transfer in brazed plate heat exchangers. *International Journal of Refrigeration*, In Press.

Osakabe, M., Hamada, T., & Horiki, S. (1999). Water flow distribution in horizontal header contaminated with bubbles. *International Journal of Multiphase Flow*, 25, 827-840.

Rouhani, S.Z., Axelsson, E. (1970). Calculation of void volume fraction in the subcooled and quality boiling regions. *International Journal of Heat and Mass Transfer*, 13, 383–393.

Vist, S., Pettersen, J. (2004). Two-phase flow distribution in compact heat exchanger manifolds. *Experimental Thermal and Fluid Science*, 28, 209–215.

Zou, Y., Hrnjak, P. (2014). Effects of fluid properties on two-phase flow and refrigerant distribution in the vertical header of a reversible microchannel heat exchanger-Comparing R245fa, R134a, R410A, and R32. *Applied Thermal Engineering*, 70, 966-976.

ACKNOWLEDGMENT

The authors thankfully acknowledge the support provided by the Air Conditioning and Refrigeration Center at the University of Illinois at Urbana-Champaign.